PROCEEDINGS OF SCIENCE

# Detection of diffuse gamma-ray emission towards a massive star forming region hosting Wolf-Rayet stars

**Kai Wang,**[a,b,*] **Hai-Ming Zhang,**[a,b] **Ruo-Yu Liu**[a,b] **and Xiang-Yu Wang**[a,b]

[a] *School of Astronomy and Space Science, Nanjing University, Nanjing 210023, Jiangsu, China*

[b] *Key laboratory of Modern Astronomy and Astrophysics(Nanjing University), Ministry of Education, Nanjing 210023, People Republic of China*

*E-mail:* k-wang@smail.nju.edu.cn

Massive star clusters hosting WR and OB-type stars have been proposed as potential Galactic cosmic-ray accelerators for decades, in particular via diffusive shock acceleration at wind termination shocks. Here we report the analysis of *Fermi* Large Area Telescope's data towards the direction of Masgomas-6a, a young massive star cluster candidate hosting two WR stars. We detect an extended $\gamma$-ray source with TS = 183 in the vicinity of Masgomas-6a, spatially coincident with two unassociated *Fermi* 4FGL sources. The $\gamma$-ray emission intensity correlates well with the distribution of molecular gas at the distance of Masgomas-6a, indicating that these gamma rays may be produced by CRs accelerated by massive stars in Masgomas-6a. At the distance of 3.9 kpc of Masgomas-6a, the luminosity of the extended source is $(1.81 \pm 0.02) \times 10^{35}$ erg s$^{-1}$. With a kinetic luminosity of $\sim 10^{37}$erg s$^{-1}$ in the stellar winds, the WR stars are capable of powering the $\gamma$-ray emission via neutral pion decay resulted from cosmic ray $pp$ interactions. The size of the GeV source and the energetic requirement suggests a CR diffusion coefficient smaller than that in the Galactic interstellar medium, indicating strong suppression of CR diffusion in the molecular cloud.

38th International Cosmic Ray Conference (ICRC2023)
26 July - 3 August, 2023
Nagoya, Japan



*Speaker





PoS(ICRC2023)835

## 1. Introduction

Ramírez Alegría et al. [1] identified two groups of massive stars aligned in the $l \sim 38°$ Galactic direction. They find more than 20 massive stars, including two Wolf-Rayets (WR122-11 and the new WR122-16), OB-type stars and one transitional object (the Luminous Blue Variable (LBV) candidate IRAS 18576+0341 [2]). The individual distances and radial velocities of these massive stars indicate two populations of massive stars in the same line of sight: Masgomas-6a and Masgomas-6b. Masgomas-6a is reported as a massive star cluster candidate with a total mass (lower limit) of $(9.0-1.3)\times10^3 M_\odot$, located at $3.9^{+0.4}_{-0.3}$ kpc, contains both Wolf-Rayets and several OB-type stars. Masgomas-6b, located at $9.6\pm0.4$ kpc, has a total mass (lower limit) of $(10.5-1.5)\times10^3 M_\odot$ and hosts a LBV candidate and an evolved population of supergiants. For both objects, the presence of evolved massive stars (the WN8-9h Wolf-Rayet in Masgomas-6a and the LBV candidate in Masgomas-6b) sets an age limit of 5 Myr [1].

In this paper, we report the detection of an extended $\gamma$-ray source towards the direction of Masgomas-6 with the *Fermi* Large Area Telescope. We also present the CO observational results of molecular clouds (MCs) in this region, using the data from the Milky Way Imaging Scroll Painting (MWISP) project, which is a multi-line survey in $^{12}$CO/$^{13}$CO/C$^{18}$O along the northern Galactic plane with the Purple Mountain Observatory (PMO) 13.7 m telescope. The correlation between the $\gamma$-ray intensity and the molecular gas at the distance of Masgomas-6a suggests that the GeV $\gamma$-ray source is likely related with the massive stars in Masgomas-6a.

## 2. *Fermi*/LAT Data Analysis

The *Fermi*-LAT is a wide field-of-view, high-energy $\gamma$-ray telescope, covering the energy range from below 20 MeV to more than 300 GeV[3]. The Pass 8 data taken from 2008 August 4 to 2022 April 9 are used to study the GeV emission towards Masgomas-6, where two *Fermi* sources (4FGL J1900.4+0339 and 4FGL J1858.0+0354) are found in the vicinity. All $\gamma$-ray photons within a $14° \times 14°$ region of interest (ROI) centered on the position of Masgomas-6 are considered for the binned maximum likelihood analysis. The publicly available software *Fermipy* (ver.1.0.1) and *Fermitools* (ver.2.0.8) are used to perform the data analysis. The event type FRONT + BACK and the instrument response functions (IRFs) ($P8R3\_SOURCE\_V3$) are used. We only consider the $\gamma$-ray events in the $3-500$ GeV energy range, with the standard data quality selection criteria "$(DATA\_QUAL > 0)\&\&(LAT\_CONFIG == 1)$". To minimize the contamination from $\gamma$-rays from the Earth limb, the maximum zenith angle is adopted to be 90°. We include all sources listed in the fourth *Fermi*-LAT catalog[6] and the diffuse Galactic interstellar emission (IEM, $gll\_iem\_v07.fits$), isotropic emission ("$iso\_P8R3\_SOURCE\_V3\_v1.txt$" ) in the background model. The spectral parameters of the sources within 4° of Masgomas-6, Galactic and isotropic diffuse emission components are all set free. The significance of $\gamma$-ray sources are estimated by maximum likelihood test statistic (TS), which is defined by TS$= -2(\ln\mathcal{L}_0 - \ln\mathcal{L}_1)$, where $\mathcal{L}_1$ and $\mathcal{L}_0$ are maximum likelihood values for the background with target source and without the target source (null hypothesis). The square root of the TS is approximately equal to the detection significance of a given source. Figure 1 shows the 3-500 GeV TS map in the the vicinity of Masgomas-6 with the binned likelihood analysis. The two 4FGL point-like sources near Masgomas-6, 4FGL

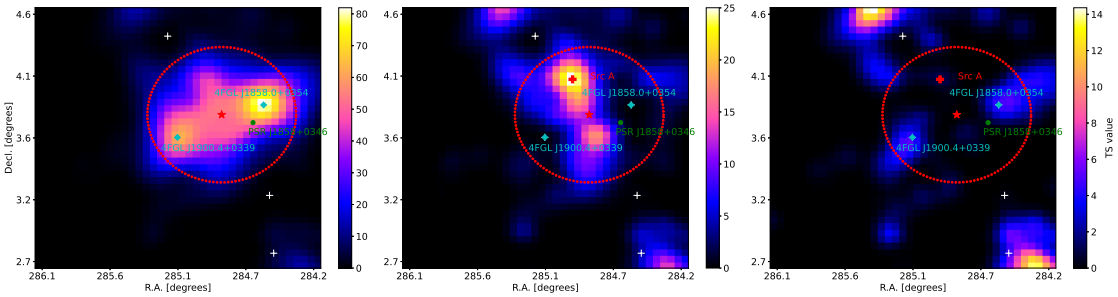


**Figure 1:** Left panel: *Fermi*-LAT TS map of the region around Masgomas-6a in 3-500 GeV. Middle panel: the residual TS map of the two point-like source model. Right panel: the residual TS map of the disk model. Background 4FGL sources are shown with white crosses. The red dashed circle shows the radius of the disk in the best-fit uniform disk model.

J1900.4+0339 and 4FGL J1858.0+0354, are located 0.16° and 0.52° away from the center of Masgomas-6, respectively. A uniform disk model and a two-dimensional (2D) Gaussian model are used to evaluate the extension. The results are shown in Table 1. We find that the uniform disk model describes well the GeV morphology, with the best-fit extension of $0.43^{+0.02^\circ}_{-0.03^\circ}$ and the best-fit position at (R.A., Decl.)=(284.81° ± 0.08°,3.84° ± 0.04°) in the energy band above 3 GeV. This position is 0.22° away from the position of Masgomas-6. The $\mathrm{TS_{ext}}$ is estimated to be 129.80 for the disk model, which is defined as $\mathrm{TS_{ext}} = 2(\ln \mathcal{L}_{\mathrm{ext}} - \ln \mathcal{L}_{\mathrm{ps}})$, where $\mathcal{L}_{ext}$ is the maximum likelihood value for the extend model and $\mathcal{L}_{ps}$ is the maximum likelihood value for the point-like model [4]. According to Ackermann et al. [4], the criterion to define a source as being extended is $\mathrm{TS_{ext}} \geq 16$ and $\mathrm{TS_{ext}} \geq \mathrm{TS_{2pts}}$ (here $\mathrm{TS_{2pts}} = 2(\ln \mathcal{L}_{\mathrm{2pts}} - \ln \mathcal{L}_{\mathrm{ps}})$ represents the improvement when adding a second point source). We find that the $\gamma$-ray source, assuming a uniform disk model, meets the criterion with $\mathrm{TS_{ext}} = 129.80$ and $\mathrm{TS_{2pts}} = 106.62$ (see Table 1). Furthermore, we compare the residual TS maps after subtracting the disk component and the two point-like source component. We find that there is bright (maximum TS ∼ 25) emission (referred to as Src A, see Figure 1) at the top left corner of the residual TS map in the two point-like source model, but the significance of this emission is significantly reduced in the disk model. This implies that the extended source model fits the GeV emission better than the two point-like sources model, consistent with our above analysis.

**Table 1:** Morphological models tested for the GeV $\gamma$-ray emission above 3 GeV.

| Morphology | R.A.(deg) | Decl.(deg) | Extension | loglikelihood | TS | $\mathrm{TS_{ext}}$ | $N_{\mathrm{dof}}$ |
|---|---|---|---|---|---|---|---|
| Null | – | – | – | 119936.52 | – | – | – |
| PS+PS | – | – | – | 120016.56 | 160.08 | – | 8 |
| Disk | 284.81 ± 0.08 | 3.84 ± 0.04 | $0.43^{+0.02}_{-0.03}$ | 120028.15 | 183.26 | 129.80 | 5 |
| Gaussian | 284.82 ± 0.04 | 3.84 ± 0.04 | 0.46 ± 0.04 | 120025.90 | 178.76 | 125.30 | 5 |

**Note:** PS+PS represents the two point source model with source positions at the two 4FGL sources. Extension in the disk and Gaussian models represents the radius containing 68% of the intensity of the tested models.

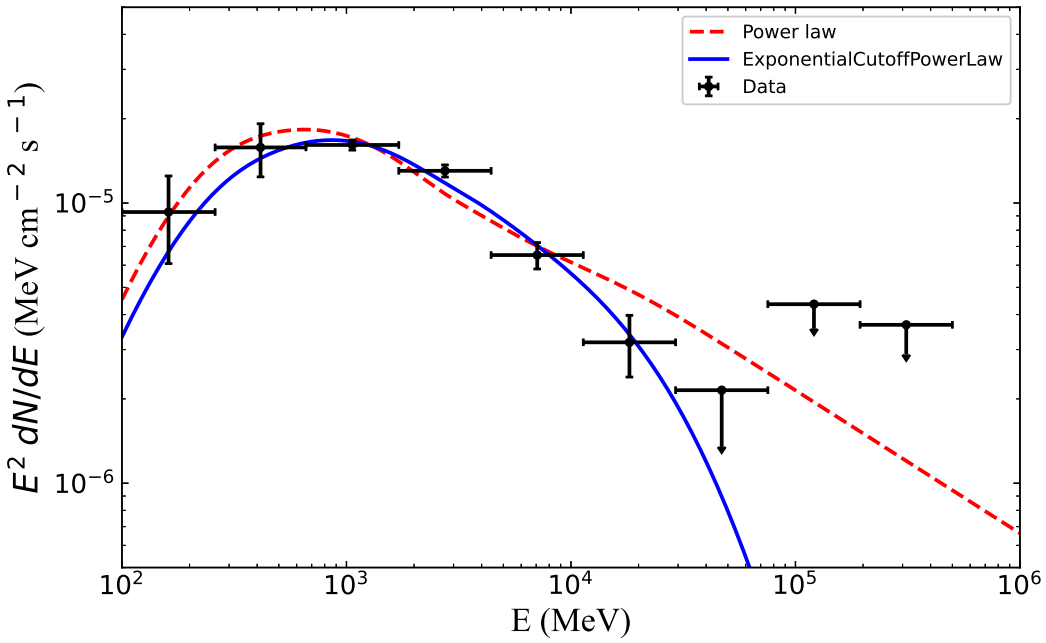


**Figure 2:** Modeling of the SED of the $\gamma$-ray source with a hadronic model. The black dots represent the *Fermi*-LAT data in 0.1-500 GeV. The red dash line represents the modeling assuming a single power-law proton spectrum. The blue solid line represents the modelling assuming a power-law with a high-energy cutoff for the proton spectrum.

The spectral energy distribution (SED) of the source in the energy band > 0.1 GeV, shown in Figure 2, is derived by *gtlike* assuming the best-fit uniform disk extension. When the TS value of spectra data point is less than 4, an upper limit is calculated at 95% confidence level using a Bayesian method [5]. Compared to a single power-law, the spectrum is better described by a log parabola empirical function $dN/dE = N_0(E/E_b)^{-(\alpha+\beta\log(E/E_b))}$. The spectral index and break energy are found to be $\alpha = 2.29 \pm 0.01$, $\beta = 0.19 \pm 0.01$ and $E_b = 1268.47 \pm 2.81$MeV. The energy flux is $(9.92 \pm 0.12) \times 10^{-11}$ erg cm$^{-2}$ s$^{-1}$ in 0.1-500 GeV. Assuming a distance of $d = 3.9$ kpc, the total $\gamma$-ray luminosity of the source in 0.1-500 GeV is $(1.81 \pm 0.02) \times 10^{35}$ erg s$^{-1}$.

## 3. CO observations

We make use of the data from the Milky Way Imaging Scroll Painting (MWISP[1]) project, which is a multi-line survey in $^{12}$CO/$^{13}$CO/C$^{18}$O observed simultaneously using the 13.7 m millimeter-wavelength telescope of the Purple Mountain Observatory at Delingha. The detailed observing strategy, the instrument, the spectral resolution, and the quality of the CO observations can be found in Su et al. [7]. In this work, we present the results of the MWISP CO survey for $2^\circ \times 2^\circ$ regions centering at $(l, b) = (37.27^\circ, -0.23^\circ)$. We estimated the kinematic distance to the MCs using the Milky Way's rotation curve suggested by Sofue [8], assuming the Sun's Galactocentric distance to be 8.0 kpc and Solar rotation velocity to be 238 km s$^{-1}$.

[1] http://english.dlh.pmo.cas.cn/ic/

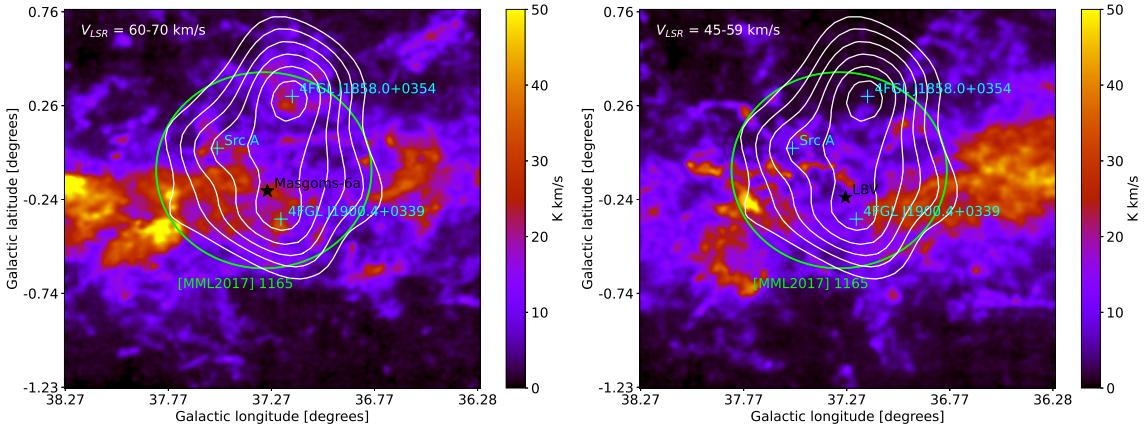


**Figure 3:** $^{12}$CO($J$=1–0) intensity map integrated in velocity range 60 – 70 km s$^{-1}$ (left panel) and 45 – 59 km s$^{-1}$ (right panel). White contours correspond to *Fermi*-LAT significance map starting from 3$\sigma$ to 8$\sigma$ by 1$\sigma$ steps. Crosses in cyan indicate the location of point sources and Src A. The green circle shows the radius of the molecular cloud "[MML2017] 1165" named by Miville-Deschênes et al. [9]. "[MML2017] 1165" is located in the velocity range of $V_{LSR}$ = (63.52 ± 6.41) km s$^{-1}$.

The distance of Masgomas-6a is estimated to be $3.9^{+0.4}_{-0.3}$ kpc [1], corresponding to a velocity $V_{\rm LSR}$ in the range of ∼ 60 – 70 km s$^{-1}$ for the MC CO emission. Note that, the velocity of each MC could indicates two candidate kinematic distances, the near side one and the far side one. The far distance of the MC in ∼ 60 – 70 km s$^{-1}$ is 8.4–9.0 kpc. The distance of Masgomas-6b is estimated to be 9.6 ± 0.4 kpc, corresponding to a velocity $V_{\rm LSR}$ in the range of ∼ 45 – 59 km s$^{-1}$. The $^{12}$CO(J = 1-0) maps for the velocity range 60 to 70 km s$^{-1}$ and 45 to 59 km s$^{-1}$ are, respectively, shown in the left and right panel of Figure 3. The intensity maps of the gamma-ray emission correlate more strongly with the gas distribution in the velocity range of 60 to 70 km s$^{-1}$. Particularly, the two point-like 4FGL sources (4FGL J1900.4+0339 and 4FGL J1858.0+0354) and Src A each coincide with one of the densest regions of the gas distribution. On the other hand, $\gamma$-ray emission intensity correlates poorly with gas distribution in the 45-59 km s$^{-1}$ velocity range compared to that in the 60-70 km s$^{-1}$ velocity range. This indicates that the extended $\gamma$-ray source is more likely to be related to Masgomas-6a.

Adopting the mean CO-to-$H_2$ mass conversion factor $X_{\rm CO} = 2 \times 10^{20}$ cm$^{-2}$ K$^{-1}$ km$^{-1}$ s [10], we estimate that the total mass of gas within the 0.52° disk of the GeV source is about $3.13 \times 10^5 d_{3.9}^2\ M_\odot$. If we assume the $\gamma$-ray emission region is spherical in geometry, then the radius is estimated to be $R \sim 36 d_{3.9}$ pc. Then the average atom density of the $H_2$ cloud in this region is about $n \simeq 70 {\rm d}_{3.9}^{-1}$ cm$^{-3}$.

## 4. Interpretation of the GeV emission

We fit the $\gamma$-ray spectra of the source with the hadronic model using the Markov Chain Monte Carlo fitting routines of Naima, a package for the calculation of nonthermal emission from relativistic particles [11]. First, we assume the parent proton spectrum is a single power-law given by $dN/dE = A(E/E_0)^{-\alpha}$. The derived parameters are $\alpha = 2.57^{+0.03}_{-0.04}$, and the total energy is $W_p = 1.81 \times 10^{49}$ erg for the protons above 1 GeV, assuming the gas density is 70 cm$^{-3}$. The

best-fit result is shown by the red dashed line in Figure 2. Below 1 GeV, the hard spectrum is due to the $\pi^0$ bump. At higher energies ($> 10$ GeV), the theoretical flux exceeds the LAT data slightly (but still within the $2\sigma$ uncertainty). This could indicate a possible cutoff in the proton spectrum around 100 GeV . Then, we consider a cutoff power-law function for the parent proton spectrum, i.e. $dN/dE = A(E/E_0)^{-\alpha}\exp(-(E/E_{\rm cut})^{\beta})$. The derived parameters are $\alpha = 2.18 \pm 0.05$ and $W_p = 1.34 \times 10^{49}$ erg for the protons above 1 GeV, if we take $\beta = 1$, $d = 3.9$ kpc, $n = 70$ cm$^{-3}$ and $E_{\rm cut} = 100$ GeV. The fitting result is shown by the blue line in Figure 2.

The young massive star cluster candidate Masgomas-6a contains two Wolf–Rayet stars and several OB-type stars. These WR stars have a mass loss rate $2 - 3 \times 10^{-5}$M$_\odot$yr$^{-1}$ and the wind velocity is $1000 - 2000$ km s$^{-1}$, so the kinetic luminosity of the stellar wind is about $10^{37}$ erg s$^{-1}$, which is sufficient to power the $\gamma$-ray emission. As the mass-loss of WR stars are quasi-continuous over the lifetime $T$, one could expect a quasi-continuous injection of CRs into the interstellar medium over the age of WR stars ($T \gtrsim 10^6$yr). The stellar wind from Masgomas-6a may drive a termination shock by interacting with the surrounding gas. The termination shock then accelerates cosmic rays, which produce gamma-ray emission by colliding with the molecular cloud.

The efficiency of production of $\gamma$-rays in the cloud is determined by the ratio between the diffusion timescale and the energy loss timescale of cosmic rays, i.e., $\eta_{pp} = t_{\rm diff}/t_{\rm pp}$. The energy loss time of cosmic ray protons colliding with the molecular gas is $t_{pp} = 1/(\sigma_{\rm pp})K_{\rm pp}nc = 10^6{\rm yr}(n/70{\rm cm}^{-3})^{-1}$, where $\sigma_{\rm pp} = 3 \times 10^{-26}$cm$^2$ is the cross section of $pp$ collisions, $K_{\rm pp} = 0.5$ is the inelasticity of pion production and $n$ is the gas number density. The diffusion time depends on the diffusion coefficient in the cloud, i.e. $t_{\rm diff} = R^2/4D$, where $R$ is the size of the source and $D$ is the diffusion coefficient. The diffusion coefficient for CRs propagating in the molecular cloud is poorly known. In the interstellar medium, the diffusion coefficient is of order of $10^{29}$cm$^2$ s$^{-1}$ for 10–100 GeV protons (see e.g. [12]) responsible for 1–10 GeV $\gamma$-rays. We assume a homogeneous diffusion coefficient and parameterize it as $D = \chi D_{\rm ISM} = \chi 10^{29}$cm$^2$ s$^{-1}$ for CRs with energy of $10 - 100$ GeV, with $\chi$ being the ratio between the CR diffusion coefficient in the cloud and the average one of the Galactic ISM. The diffusion time is then given by $t_{\rm diff} = 10^3\chi^{-1}(D_{\rm ISM}/10^{29}{\rm cm}^2\ {\rm s}^{-1})^{-1}$ yr for $R = 36$ pc. Thus, the required CR injection rate to power the $\gamma$-ray emission is $L_p = L_\gamma/\eta_{pp} = 1.8 \times 10^{38}\chi$ erg s$^{-1}$. To account for the CR injection rate with the stellar wind power of WRs, $\chi \lesssim 0.1$ is required for a reasonable CR acceleration efficiency, implying that the diffusion coefficient is significantly suppressed in the molecular cloud. We also note that a significant part of CRs could have already escaped out of the $\gamma$-ray emission region. The relation between the total injected CR energy and the CR energy remained in the $\gamma$-ray emission region can be expressed as $L_{\rm p,tot}/L_p = (r_{\rm diff}/R)^2 = 100(\chi/0.1)(T/10^6{\rm yr})$, where $r_{\rm diff}$ is the the total diffusion length of CRs corresponding to the age $T$ of the WR stars.

## 5. Summary

We analyzed the *Fermi* Large Area Telescope's data towards the direction of Masgomas-6a. An extended $\gamma$-ray source with a radius of 0.52 degree is found in the vicinity of Masgomas-6a. Our analysis shows a correlation between the intensity of $\gamma$-ray emission and the density of molecular gas in the region. Combined with the fact that the distance of the molecular cloud inferred from the velocity distribution is consistent with that of Masgomas-6a, the correlation indicates that the $\gamma$-ray

emission is related with Masgomas-6a. A natural scenario is that the two WR stars in Masgomas-6a accelerate cosmic rays, which produce the $\gamma$-ray emission through inelastic proton-proton collisions with the molecular gas. With a kinetic luminosity of $\sim 10^{37}$erg s$^{-1}$ in the stellar winds, the two WR stars are capable of powering the $\gamma$-ray emission.

## Acknowledgments

This work was supported by the National Key R&D program of China under the grant 2018YFA0404203, the NSFC grants 12121003 and U2031105, the Natural Science Foundation of Jiangsu Province grant BK20220757, and China Manned Spaced Project (CMS-CSST-2021-B11). This research made use of the data from the Milky Way Imaging Scroll Painting (MWISP) project. We are grateful to all the members of the MWISP working group. Thanks to NASA Fermi Collaboration for providing the excellent data and tools that made this work possible.

## References

[1] Ramírez Alegría, S., Herrero, A., Rübke, K., et al. 2018, A&A, 614, A116. doi:10.1051/0004-6361/201731720

[2] Pasquali, A. & Comerón, F. 2002, A&A, 382, 1005. doi:10.1051/0004-6361:20011667

[3] Atwood, W. B., Abdo, A. A., Ackermann, M., et al. 2009, ApJ, 697, 1071. doi:10.1088/0004-637X/697/2/1071

[4] Ackermann, M., Ajello, M., Baldini, L., et al. 2017, ApJ, 843, 139. doi:10.3847/1538-4357/aa775a

[5] Helene, O. 1983, Nuclear Instruments and Methods in Physics Research, 212, 319. doi:10.1016/0167-5087(83)90709-3

[6] Abdollahi, S., Acero, F., Ackermann, M., et al. 2020, ApJS, 247, 33. doi:10.3847/1538-4365/ab6bcb

[7] Su, Y., Yang, J., Zhang, S., et al. 2019, ApJS, 240, 9. doi:10.3847/1538-4365/aaf1c8

[8] Sofue, Y. 2015, PASJ, 67, 75. doi:10.1093/pasj/psv042

[9] Miville-Deschênes, M.-A., Murray, N., & Lee, E. J. 2017, ApJ, 834, 57. doi:10.3847/1538-4357/834/1/57

[10] Bolatto, A. D., Wolfire, M., & Leroy, A. K. 2013, ARA&A, 51, 207. doi:10.1146/annurev-astro-082812-140944

[11] Zabalza, V. 2015, 34th International Cosmic Ray Conference (ICRC2015), 34, 922

[12] Strong, A. W., Moskalenko, I. V., & Ptuskin, V. S. 2007, Annual Review of Nuclear and Particle Science, 57, 285. doi:10.1146/annurev.nucl.57.090506.123011